Chinese Chemical Letters 33 (2022) 3193–3196

Contents lists available at ScienceDirect

Chinese Chemical Letters

journal homepage: www.elsevier.com/locate/cclet

Fluorescent polymer-modified gold nanobipyramids for temperature sensing during photothermal therapy in living cells

Juan Qiao[a,b], Xiangfei Li[a,c], Li Qi[a,b,*]

[a] Beijing National Laboratory of Molecular Sciences, Key Laboratory of Analytical Chemistry for Living Biosystems, Institute of Chemistry, Chinese Academy of Sciences, Beijing 100190, China
[b] School of Chemical Sciences, University of Chinese Academy of Sciences, Beijing 100049, China
[c] College of Chemical and Pharmaceutical Engineering, Hebei University of Science and Technology, Shijiazhuang 050018, China

ARTICLE INFO

Article history:
Received 6 September 2021
Revised 4 November 2021
Accepted 26 December 2021
Available online 1 January 2022

Keywords:
Fluorescent polymer
Gold nanobipyramids
Temperature monitoring
Photothermal therapy

ABSTRACT

The temperature monitoring of treated cancer cells is critical in photothermal therapy. Current methods of detecting intracellular temperatures have low accuracy and poor spatial resolution, which limits their application to photothermal therapy. Herein, a strategy for targeted recognition and selective capture of MCF-7 breast cancer cells based on fluorescent polymer poly(*N*-isopropylacrylamide-benzoxadiazole-2-vinyl-4,4-dimethyl azlactone, PNMV) and modified gold nanobipyramids (AuNBPs-PNMV) was developed for temperature sensing during photothermal therapy. A mucin-1 protein aptamer (Apt) was applied to selectively target mucin-1 protein overexpressed on the surfaces of the MCF-7 cells, which can reduce interference by affinity interaction between the Apt and proteins. During photothermal therapy, the significant AuNBPs photothermal effect increases the fluorescence intensity of PNMV with temperature. Irradiation of MCF-7 cells cultured with AuNBPs-PNMV@Apt by an 808 nm laser increases the temperature of the system, while the cells can be inactivated because of the remarkable AuNBPs-PNMV@Apt photothermal effect. The results indicate that variation in the fluorescence of AuNBPs-PNMV@Apt can be applied as thermometers to monitor the intracellular effect of photothermal therapy.

Temperature, as one of the most significant physiological conditions, is important for function and biochemical reactions of cell. Photothermal therapy (PTT) involves introducing a photothermal conversion material to tissues, where it absorbs light and generates heat to kill target tumor cells. During PTT, it is expected to realize high therapeutic accuracy and less injury to normal tissues [1,2]. Currently, various effective materials have been applied to PTT, including metallic nanoparticles (Pd and Au) [3,4], carbon materials [5,6], and metal sulfides and oxides [7,8].

Generally, laser radiation time and cell exposure power are the most significant factors in PTT, as they determine the damage caused to normal cells surrounding targeted lesions. Generally, the cancer cells can be permanently inactivated by temperatures greater than 43 °C [9]. These studies have focused on certain effects of PTT, such as the cancer cells survival rate and the diseased tissues disappearance or recurrence. However, the main problem in using PTT against cancer cells is to determine the temperature to which tumors can be heated while keeping PTT. Excessive thermal transfer can affect normal tissues near lesions and residual cancer cells, which may harm healthy cells and cause insufficient inactivation of the tumor. Consequently, normal cells may be damaged while residual cancer cells may become more likely to grow. Therefore, a system for accurate, real-time, intracellular temperature sensing is required to provide useful overheating information during PTT experiments.

There have been many reports of measuring intracellular temperatures using fluorescent molecular thermometers [10,11], which may comprise inorganic nanoparticles [12,13], nanodiamonds [14] and dye-modified polymeric particles [15–17]. However, current technology for temperature measurement during PTT experiments has the following disadvantages. (i) The temperature sensing material is not always combined with PTT nanoparticles, which may cause difficulty in measuring the distribution of and change in cancer cell temperatures as well as the boundary of normal cells during PTT [18]. (ii) Some of the reported thermometers based on fluorescent molecular possess the same fluorescence emission wavelength as cell self-emissions, especially during the photothermal killing of cancer cells. Thus, a bifunctional material that integrates temperature measurement and PTT will be benefi-

* Corresponding author at: Beijing National Laboratory of Molecular Sciences, Key Laboratory of Analytical Chemistry for Living Biosystems, Institute of Chemistry, Chinese Academy of Sciences, Beijing 100190, China
E-mail address: qili@iccas.ac.cn (L. Qi).

https://doi.org/10.1016/j.cclet.2021.12.070
1001-8417/

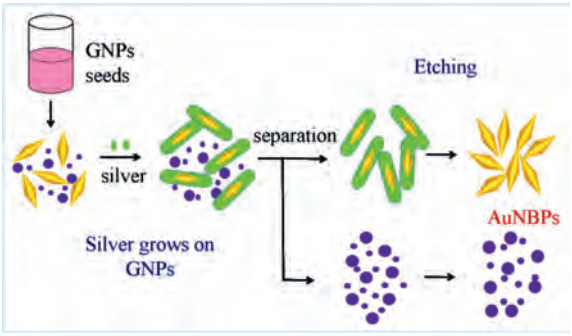

Fig. 1. Schematic illustration of the AuNBPs purification steps.

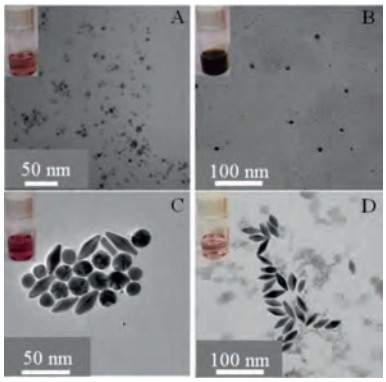

Fig. 2. TEM images of the as-grown AuNPs seeds (A), bimetallic Au/Ag products (B), Au/Ag heteronanorods (C), and AuNBPs (D).

cial to more safe and effective PTT. Such a material could give high-resolution-spatial temperature sensing as well as real-time and accurate thermal feedback in the process of PTT.

In order to solve the above problem, a suitable auxiliary tool is needed to measure intracellular temperatures. The fluorescent polymeric thermometers contained fluorescent molecules and polymers, which are promising materials for temperature monitoring and mapping in living cells, as they worked at the molecular level. Moreover, many thermo-responsive polymers have been utilized as sensors, drug carriers, catalyst supports, and bio-separation materials in many fields [19–21]. Gold nanobipyramids (AuNBPs) have two atomically sharp tips and exhibit extremely strong electric field enhancement [22], and have attracted increasing attention recently. Compared with the other gold nanomaterials, AuNBPs possess well size homogeneity and better shape, tunable absorption wavelengths and good chemical stability. The absorption wavelengths of AuNBPs can easily be tuned to the near-infrared (NIR) region during synthesis by controlling their aspect ratio. In the NIR region, strong optical absorption gives AuNBPs the potential to act as a hyperthermia agent for PTT, in which ranging living tissue has a less absorption [23]. Targeting ligands have also been introduced onto thermo-responsive polymers to achieve *in vivo* tumor tissues targeting. By modifying targeting groups such as single-chain fragments of antibodies, antibodies, or peptide sequences, AuNBPs would be introduced into tumor cells, causing to an excellent therapeutic result [24–26]. In particular, mucin-1 protein has been used for targeting breast cancer because it was found to be over-expressed in most of the breast carcinomas of human [27].

In the present study, a unique recognition method for the selectively capturing of human breast cancer cells was developed for PTT. It is based on AuNBPs-poly(*N*-isopropylacrylamide-2-vinyl-4,4-dimethyl azlactone)@mucin-1 protein aptamers (PNMV@Apt). The thermo-sensitive PNMV combined with a fluorescent dye can change fluorescence intensity considerably with temperature. For efficiently and selectively capturing of breast cancer cells, Apt-functioned nanoparticles were prepared and applied to distinguish MCF-7 breast cancer cells from complex biosamples. Furthermore, for combination the thermo-sensitive moiety with Apt part, a special monomer (V) as linker was copolymerized onto the temperature sensing fluorescent polymer. Accordingly, by decorating PNMV@Apt onto the surfaces of AuNBPs, a bifunctional material for synchronous temperature measurement and PTT was created

Typically, the prepared AuNBPs were formed of two pentagonal pyramids connected at their bases. AuNBPs were selected as a photothermal material due to their good plasmon resonance property and tunable longitudinal plasmon resonance wavelengths. The AuNBPs were synthesized by a silver-assisted seeded growth method [28,29]. The processes for preparation and purification method of the AuNBPs are displayed in Fig. 1. Representative TEM images show the morphologies of the as-grown AuNBP sample (Fig. 2A), bimetallic Au/Ag products (Fig. 2B), Au/Ag heteronanorods (Fig. 2C) and AuNBPs (Fig. 2D). The results show that the as-synthesized nanoparticles are consistent with the characteristics of nanoparticles in different stages.

The absorption spectra of AuNBPs synthesized under different conditions were investigated. The results show that the longitudinal plasmon resonance wavelengths (LPRWs) of the AuNBPs could be tailored to the visible to NIR regions by varying the volumes of the seed solutions (Fig. S1 in Supporting information). The AuNBPs had two obvious plasmonic dominant peaks related to the transverse localized surface plasmon resonance mode in high-energy region and in low-energy region. Furthermore, the LPRWs of the AuNBPs were determined by the UV–vis absorption spectrum to be approximately 780 nm, which is a good match for the 808 nm laser applied for an efficient photothermal effect. The morphology of the AuNBPs was observed by TEM (Fig. 2), which showed them to have a uniform size of length = 39.20 nm and width = 16.53 nm (Fig. 2D).

Well-defined thermo-responsive PNM- and PNMV-bearing fluorophores with molecular weights of 1.06×10^4 and 1.16×10^4 (PDIs of 1.3 and 1.4), respectively, were synthesized *via* reversible addition-fragmentation chain transfer (RAFT) polymerization (Table S1 in Supporting information). The PNMV synthesis process is displayed in Figs. S2–S4 (Supporting information). Compared with the FT-IR spectrum of PNM, Fig. S5 (Supporting information) shows the signal of azlactone rings of V moiety at 1265 cm^{-1} (C–O–C stretching) [30], which confirm the copolymerization of PNM and V. The compositions of PNM and PNMV were also characterized by ^1H NMR spectroscopy (Fig. S6 in Supporting information). The presence of –CH proton resonances at 3.90 ppm and $-CH_3$ proton resonances at 0.90–1.20 ppm indicate the NM block of the polymer PNM and PNMV. The $-CH_3$ proton resonances of the V monomer at 1.10 ppm would overlap with the $-CH_3$ proton resonances of PNM, which caused no obvious difference between the two spectra.

Owing to their design, the AuNBPs were chosen to serve as a photothermal reagent with the PNMV functioning as a thermometer. Thus, the PNMV was immobilized onto the AuNBPs using the thiol group in the polymer. Firstly, the fluorescence responses of AuNBPs-PNMV@Apt to temperature changing were studied to verify its thermo-responsive property. The fluorescence spectrum of AuNBPs-PNMV@Apt emission at 550 nm in the 34.0–50.0 °C temperature range was obtained (Fig. 3A). The data show that the fluorescence intensity of AuNBPs-PNMV@Apt at 550 nm increases with temperature. The average fluorescence intensity of AuNBPs-PNMV@Apt changed linearly with temperatures of 36.0–47.0 °C, with a correlation coefficient of 0.976 (Fig. S7 in Supporting information). Variation in the diameter of AuNBPs-PNMV@Apt with in-

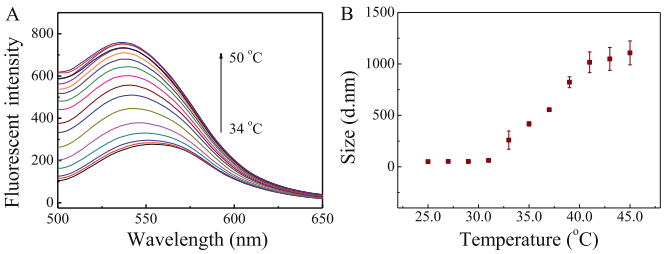

Fig. 3. Effect of temperature on the fluorescence intensity of AuNBPs-PNMV@Apt (A) and DLS results of the AuNBPs-PNMV@Apt (B).

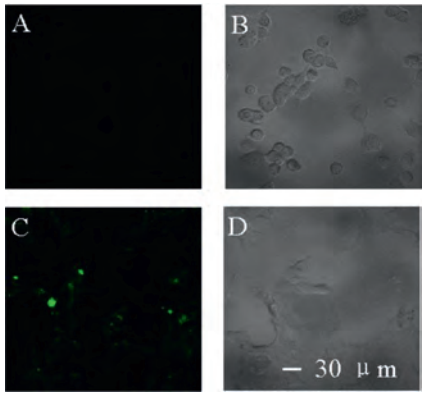

Fig. 4. Fluorescence images of COS-7 (A, B) and MCF-7 (C, D) obtained after incubation with AuNBPs-PNMV@Apt. Scale bars in A, B, C and D: 30 μm.

creasing temperature was detected by DLS. The diameter increased with temperature, from 49.9 nm at 25 °C to 1107.5 nm at 45 °C (Fig. 3B). These results demonstrate that the fluorescence intensity of the AuNBPs-PNMV@Apt can indicate temperature during their photothermal conversion.

For cancer cell targeting, mucin-1 protein aptamer was anchored onto the surfaces of AuNBPs-PNMV through interactions with V and amino groups. The resulting AuNBPs-PNMV@Apt was applied as a targeting tool to achieve selective recognition of mucin-1 protein over-expressed MCF-7 cells. To further study the selectivity of this method for the distinguishing of MCF-7 cells, measurements were performed using MCF-7 and COS-7 cells, respectively. As illustrated in Fig. 4, the presence of target MCF-7 cells resulted in a more significant fluorescence intensity increase than that of COS-7 cells. This comparison illustrates the good selectivity of the target recognition assay, which can be attributed to recognition by the mucin-1 protein aptamer.

Fluorescence imaging of temperature changing in living cells was carried out using MCF-7 cells incubated with AuNBPs-PNMV@Apt. A representative fluorescence image with a temperature increase of 25.0 °C to 41.9 °C is observed in Fig. 5A. The imaging reveals that the fluorescence intensity of MCF-7 cells had a characteristic temperature-dependent property, which given an excellent linear calibration curve (Fig. 5B, $y = 1.8x - 37.9$) to be fitted in the range of 28.0–43.5 °C with a correlation coefficient of 0.928. The solid line indicates the linear fit with a slope of 1.3%/°C, which displayed a well sensitivity of this probe.

A standard cell toxicity determination was used to analyze the cytotoxicity of AuNBPs-PNMV@Apt before they were applied in further biological investigation. Fig. S8 (Supporting information) shows the cell viability of MCF-7 cancer cells after 4 h incubation with different concentrations of AuNBPs-PNMV@Apt. The results show that even when the concentration of AuNBPs-PNMV@Apt increased to 1.0 mg/mL, the viability of MCF-7 cells was still > 92.0%, indicating that AuNBPs-PNMV@Apt pose negligible toxicity to MCF-

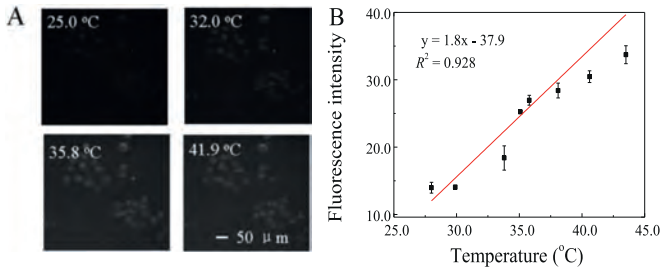

Fig. 5. (A) Fluorescence images of MCF-7 cells got at 25.0, 32.0, 35.8 and 41.9 °C. Scale bars: 50 μm. (B) Temperature-dependent calibration curve of AuNBPs-PNMV@Apt fluorescence intensity. The fluorescence intensity in living cells was got from images of MCF-7 cells.

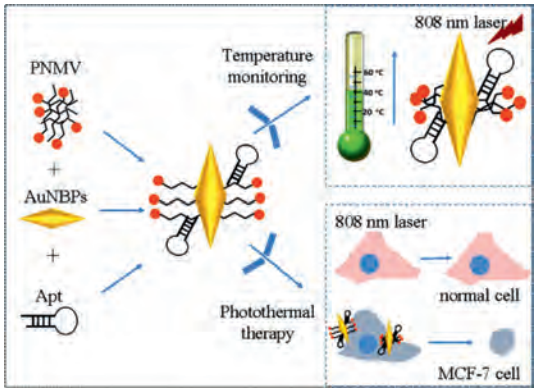

Fig. 6. Schematic diagram of the proposed AuNBPs-PNMV@Apt for measurement of the intracellular temperature during the tumor cells photothermal therapy.

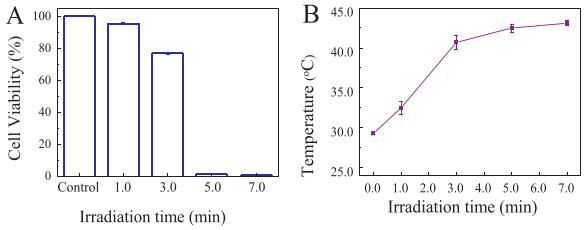

Fig. 7. (A) The state of MCF-7 cells (alive or dead) in the control sample and the sample incubated with AuNBPs-PNMV@Apt under irradiation by an 808 nm laser for different durations. (B) Temperature variation curves were measured from MCF-7 cells labeled with AuNBPs-PNMV@Apt during different durations of 808 nm laser exposure.

7 cells at the doses studied in this work. The fluorescence intensity of the AuNBPs@PNIPAM preserved in buffer solution simulated the *in vivo* conditions (200.0 mmol/L KCl, 2.0 mg/mL BSA at pH 7.5) for 24 h was investigated. The results displayed that the fluorescence intensity remained almost unchanged (RSD = 2.3%), indicating the stability of current system *in vivo* was good for at least 24 h and showing great potential for applying *in-vivo* temperature sensing during skin cancer PTT process.

On the bases of the above results, the intracellular PTT effect of AuNBPs-PNMV@Apt was investigated further (Fig. 6). MCF-7 cells were exposed to an 808 nm laser with a power density of 2.2 W/cm^2 after incubated with AuNBPs-PNMV@Apt. By the irradiation time variation, the states of the MCF-7 cells (alive or dead) in the control sample and the one incubated with AuNBPs-PNMV@Apt were also measured (Fig. 7A). The live MCF-7 cells in the control sample hardly decreased, but those incubated with AuNBPs-PNMV@Apt decreased to 95.53%, 77.02%, 1.35% and 0.91% after irradiation times of 1.0, 3.0, 5.0 and 7.0 min, respectively. These *in vitro* CCK-8 assay results clearly indicate that AuNBPs-

PNMV@Apt can take the role of a good hyperthermia material for *in vitro* PTT under irradiation by an 808 nm laser. The above experimental results give us the chance to further investigate the temperature changing process during PTT. It is important to know how the temperature of AuNBPs-labeled cells changes by 808 nm laser irradiation. The temperature changes resulting from the photothermal killing of targeted MCF-7 cells were determined from fluorescence images. The results (Fig. 7B) imply that the temperature of the MCF-7 cells significantly increased with 808 nm laser irradiation times of 0 min to 7.0 min. At 3.0 min, the final temperature exceeded 40.7 °C and kept steady rised to 43.1 °C in the following 4 min, meaning that the heat conduction from AuNBPs reached equilibrium with the surrounding circumstances. This also meant the AuNBPs can generate enough heat to kill MCF-7 cancer cells within a certain period of time. Because this form of PTT operates at the microscale, it is strongly dependent on the thermal propagation range and laser irradiation time. This result also corresponds to the PTT effects at different times in Fig. 7A. Moreover, an IR thermal imaging-based methodology has been used for monitoring the temperature variation in MCF-7 breast cancer cells during PTT (Fig. S9 in Supporting information). In this sense, our AuNBPs-PNMV@Apt-based temperature measurement approach shows promise for precisely monitoring the temperatures at the micro scale level during PTT. Table S2 (Supporting information) shows the comparison between the reported and the proposed gold nano-materials for temperature measurement. It has been found that the AuNBPs-PNMV@Apt not only could be easily synthesized, but also performed well in intracellular temperature sensing and cells targeting.

In summary, a facile and feasible method for temperature sensing was constructed during the photothermal therapy of AuNBPs-PNMV@Apt-labeled tumor cells. By modifying high-specificity and -affinity mucin-1 protein aptamer on the surfaces of AuNBPs-PNMV, a high photothermal conversion efficiency material was obtained that can kill tumor cells under 808 nm laser irradiation. During photothermal therapy of MCF-7 cancer cells labelled with AuNBPs-PNMV@Apt, temperature variation during the photothermal process can be monitored continuously because of the excellent photothermal effect of the AuNBPs and the thermosensitive property of fluorescence PNMV from the AuNBPs-PNMV@Apt. This method is able to monitor temperature changes during the photothermal therapy of cells, and provides a more precise PTT strategy. This method will help to avoid damage to non-labeled normal cells and achieve effective PTT under moderate conditions. Moreover, it is proved that the targeting AuNBPs-PNMV@Apt is valuable as a novel, low-risk, and theranostic material for PTT in breast cancer.

Declaration of competing interest

There are no conflicts of interest.

Acknowledgments

The authors are grateful for the financial support from the National Natural Science Foundation of China (Nos. 22074148, 21874138, 21635008, 21727809).

Supplementary materials

Supplementary material associated with this article can be found, in the online version, at doi:10.1016/j.cclet.2021.12.070.

References

[1] Y.Z. Wang, Y.J. Song, G.X. Zhu, et al., Chin. Chem. Lett. 29 (2018) 1685–1688.
[2] M.M. Hou, Y.X. Zhong, L. Zhang, et al., Chin. Chem. Lett. 32 (2021) 1055–1060.
[3] X. Chen, Z.N. Liu, S.G. Parker, et al., ACS Appl. Mater. Interfaces 8 (2016) 15857–15863.
[4] Y.H. Liu, Z.W. Li, Z.B. Yin, et al., ACS Appl. Mater. Interfaces 12 (2020) 14866–14875.
[5] L.H. Peng, Y.H. Zhang, L.J. Han, et al., ACS Appl. Mater. Interfaces 7 (2015) 18628–18637.
[6] J.T. Robinson, S.M. Tabakman, Y. Liang, et al., J. Am. Chem. Soc. 133 (2011) 6825–6831.
[7] J. Cui, R. Jiang, C. Guo, et al., J. Am. Chem. Soc. 140 (2018) 5890–5894.
[8] A. Riedinger, T. Avellini, A. Curcio, et al., J. Am. Chem. Soc. 137 (2015) 15145–15151.
[9] D. Jaque, L. Martinez Maestro, B. del Rosal, et al., Nanoscale 6 (2014) 9494–9530.
[10] J. Qiao, X.Y. Mu, L. Qi, Biosen. Bioelectron. 85 (2016) 403–413.
[11] X.F. Z.hao, W.L. Gao, J.W. Yin, et al., Talanta 226 (2021) 122101.
[12] H. Fischer, G.S. Harms, O.S. Wolfbeis, Angew. Chem. Int. Ed. 50 (2011) 4546–4551.
[13] Z.Y. Wang, X.Q. Ma, S.F. Zong, et al., Talanta 131 (2015) 259–265.
[14] G. Kucsko, P.C. Maurer, N.Y. Yao, et al., Nature 500 (2013) 54–58.
[15] Y. Takei, S. Arai, A. Murata, et al., ACS Nano 8 (2014) 198–206.
[16] K. Okabe, N. Inada, C. Gota, Y, et al., Nat. Commun. 3 (2012) 705.
[17] C.Y. Chen, C.T. Chen, Chem. Commun. 47 (2011) 994–996.
[18] Y.F. Kang, B. Zheng, C.Y. Li, et al., Anal. Chem. 92 (2020) 1292–1300.
[19] L.A. Lyon, Z. Meng, N. Singh, et al., Chem. Soc. Rev. 38 (2009) 865–874.
[20] C. Weber, R. Hoogenboom, U.S. Schubert, Prog. Polym. Sci. 37 (2012) 686–714.
[21] M.L. Wei, Y.F. Gao, X. Li, et al., Polym. Chem. 8 (2017) 127–143.
[22] J. Wang, H. Zhang, X. Xiao, et al., Acta Biomater. 107 (2020) 260–271.
[23] J. Feng, L.M. Chen, Y.Z. Xia, et al., ACS Biomater. Sci. Eng. 3 (2017) 608–618.
[24] H. Yang, H.P. He, Z.R. Tong, et al., J. Colloid Interface Sci. 565 (2020) 186–196.
[25] L.H. Peng, Y.H. Zhang, L.J. Han, et al., ACS Appl. Mater. Intertfaces 7 (2015) 18628–18637.
[26] Z.W. Mao, R. Cartier, A. Hohl, et al., Nano Lett. 11 (2011) 2152–2156.
[27] E.A. Rakha, R.W.G. Boyce, D. Abd El-Rehim, Mod. Pathol. 18 (2005) 1295–1304.
[28] X.K. Wu, L.X. Mu, M. Chen, et al., ACS Appl. Bio Mater. 6 (2019) 2668–2675.
[29] T.H. Chow, N.N. Li, X.P. Bai, et al., Acc. Chem. Res. 52 (2019) 2136–2146.
[30] Y. Praiin, K. Tankanya, B. Rutnakornpituk, et al., Polymer (Guildf) 53 (2012) 113–120.